



OPEN

Input dependent modulation of olfactory bulb activity by HDB GABAergic projections

Erik Böhm, Daniela Brunert & Markus Rothermel  

Basal forebrain modulation of central circuits is associated with active sensation, attention, and learning. While cholinergic modulations have been studied extensively the effect of non-cholinergic basal forebrain subpopulations on sensory processing remains largely unclear. Here, we directly compare optogenetic manipulation effects of two major basal forebrain subpopulations on principal neuron activity in an early sensory processing area, i.e. mitral/tufted cells (MTCs) in the olfactory bulb. In contrast to cholinergic projections, which consistently increased MTC firing, activation of GABAergic fibers from basal forebrain to the olfactory bulb leads to differential modulation effects: while spontaneous MTC activity is mainly inhibited, odor-evoked firing is predominantly enhanced. Moreover, sniff-triggered averages revealed an enhancement of maximal sniff evoked firing amplitude and an inhibition of firing rates outside the maximal sniff phase. These findings demonstrate that GABAergic neuromodulation affects MTC firing in a bimodal, sensory-input dependent way, suggesting that GABAergic basal forebrain modulation could be an important factor in attention mediated filtering of sensory information to the brain.

The basal forebrain (BF) is a complex of subcortical nuclei with projections to various brain areas and has been implicated in attention and cognitive control. It constitutes the primary source of cholinergic projections to limbic structures, the cortical mantle, and olfactory areas¹. Cholinergic neuromodulatory systems are thought to enhance sensory processing and amplify the signal-to-noise ratio of relevant responses²⁻⁵ e.g. the running-induced gain increases evident in sensory cortex^{6,7} or the dishabituation of odor responses in the olfactory system⁸. Furthermore, they have been identified as key players in mediating attentional modulation of sensory processing as well as in coordinating cognitive operations^{9,10}. However, the concept of a prevalent role of cholinergic cells in the BF was recently challenged as the activity of non-cholinergic neurons was shown to strongly correlate with arousal and attention¹¹⁻¹⁵. Despite the knowledge of BF subpopulations containing neurotransmitters different from acetylcholine¹⁶⁻¹⁹ no direct comparison of modulation effects caused by cholinergic and non-cholinergic projections is currently available. Especially for sensory processing which is strongly influenced by attentional states²⁰, the effects of non-cholinergic BF modulation have been sparsely investigated.

The olfactory system in mice is heavily innervated by centrifugal inputs from the BF with the majority of bulbopetal neurons located in the horizontal limb of the diagonal band of Broca (HDB)²¹⁻²⁶. Though only about one-fifth of BF neurons are cholinergic²⁵ studies on olfactory processing have mainly focused on cholinergic effects^{8,27-45}. In *in vivo* studies, a specific activation of cholinergic HDB cell bodies was shown to inhibit spontaneous mitral tufted cell activity²⁷ while optogenetically activating cholinergic axons directly in the OB added an excitatory bias to OB output neurons: the enhancement of mitral/tufted cell odorant responses occurred independently of the strength or even polarity of the odorant-evoked response²⁸. The effect of cholinergic fiber stimulation is reminiscent of sensory gain modulation in the form of baseline control¹⁶, which fits well to behavioral effects of nicotinic acetylcholine modulation in the OB³⁶ reported to increase behavioral discriminability.

Despite 30% of the bulbopetal projections neurons in the BF being GAD-(glutamic acid decarboxylase, the rate-limiting enzyme in the synthesis of GABA) positive²⁵, less attention has been directed towards GABAergic BF OB projections^{23,47,48}. Using predominantly *in vitro* OB slice recordings, studies identified periglomerular interneurons⁴⁸ and granule cells⁴⁷ as targets of GABAergic projection.

Here, we used electrophysiological and optogenetic approaches to examine how cholinergic or GABAergic projections from BF modulate MTC output from the OB *in vivo*. We found marked differences between these

Department of Chemosensation, AG Neuromodulation, Institute for Biology II, RWTH Aachen University, Aachen, 52074, Germany. ✉e-mail: m.rothermel@sensorik.rwth-aachen.de

projections; centrifugal cholinergic fibers from BF lead to an enhanced excitation of MTCs both at rest and in response to weak or strong sensory inputs. Effects of GABAergic BF axon stimulation in the OB on the other hand were sensory input strength dependent and mainly caused suppression of spontaneous MTC activity while predominantly enhancing odor-evoked MTC spiking.

These results suggest that both, cholinergic and GABAergic projections from the same area, rapidly modulate sensory output but might have markedly different impacts on sensory information processing.

Results

Differential expression of Chr2 in basal forebrain projection neurons. To selectively target cholinergic or GABAergic projections from BF to the OB we used mouse lines expressing Cre under control of the ChAT (ChAT-Cre mice;⁴⁹) or the GAD2 promoter (GAD2-Cre;⁵⁰). We expressed channelrhodopsin specifically in cholinergic or GABAergic BF neurons using a Cre-dependent viral expression vector targeted to BF by stereotaxic injection (Supp. Fig. 1). As reported previously^{28,51,52} viral injection in ChAT-Cre animals led to Chr2-EYFP expression in the somata and processes of neurons throughout HDB and, to a lesser extent, the vertical limb of the diagonal band of Broca (Fig. 1A). In few preparations sparsely labeled neurons could be additionally observed in the magnocellular preoptic nucleus (MCPO, data not shown). BF-injected GAD2-Cre animals displayed Chr2-EYFP expression predominantly in the HDB (Fig. 1B). In fewer cases, the MCPO showed a sparser cellular expression. To examine the extent of overlap between GABAergic and cholinergic cells in HDB we labeled sections from transgenic GAD-GCaMP6 mice with antibodies against vesicular acetylcholine transporter (VAcHT) (Fig. 1C). Immunostaining revealed that $7.9 \pm 5\%$ ($n = 2$ mice, 635 cells) of GCaMP-positive cells showed additional labeling for VAcHT. Though we cannot completely exclude that the 7.9% of cells co-labeled with VAcHT could be, partially or completely, bulbopetal neurons, we took this finding as a basis for a differential functional analysis of GABAergic and cholinergic projections in the OB.

Four weeks after virus infection of Cre expressing mice, Chr2-EYFP protein was apparent in BF fibers throughout the OB (Fig. 1D). In ChAT-Cre mice labeled axon terminals were visible in all layers of the OB (Fig. 1D left, Fig. 1E), consistent with earlier reports about cholinergic fiber distribution^{25,28,53–56}. The fluorescence intensity of EYFP per area unit was uniform across superficial OB layers and declined in the granule cell layer. In GAD2-Cre animals, the OB was also densely innervated by labeled fibers. Here, the fluorescence intensity per area unit was especially high in the glomerular and the granule cell layer (Fig. 1D right, Fig. 1E) recapitulating previous findings⁴⁷ but also strong in the mitral cell layer. Fluorescence intensities were distinctly lower in the external plexiform layer, the main location of MTC / GC dendrodendritic synapses. The normalized fluorescence intensity per area unit of single fibers in ChAT-Cre and GAD-Cre OB was not significantly different (1.00 ± 0.06 and 1.06 ± 0.06 , respectively; $n = 3$ mice, $p = 0.52$). Therefore, the differences in average fluorescence intensities reflect the difference in fiber density rather than Chr2-EYFP expression levels.

Optogenetic activation of cholinergic and GABAergic axons in the OB modulates MTC spontaneous spiking. To investigate BF modulation effects on early olfactory processing, we directed 473 nm light (1–10 mW total power) onto the dorsal OB surface while recording multi-channel electrical activity from dorsally located presumptive MTCs in anesthetized, double-tracheotomized mice (Fig. 1F–H) (see Materials and Methods).

To assess the impact of cholinergic and GABAergic fiber stimulation on MTC excitability in the absence of sensory input, we optically activated BF axons without ongoing inhalation (Fig. 2A). In this condition, MTC display an irregular firing pattern^{28,57,58}. As shown previously²⁸, optogenetic activation of cholinergic fibers in ChAT-Cre mice leads to a significant increase of spontaneous MTC spiking from 2.05 ± 2.34 Hz (mean \pm SD) before stimulation to 2.40 ± 2.24 Hz during stimulation ($n = 27$ units from 5 mice; $p = 0.0157$ Wilcoxon signed rank test). 8 of these units (30%) showed a significant stimulation-evoked increase in firing activity when tested on a unit-by-unit basis (Mann–Whitney U test); none showed a decrease (Fig. 2B, left).

In contrast, optical stimulation in GAD2-Cre mice led to a significant decrease in MTC spontaneous spiking, from 5.43 ± 4.07 Hz (mean \pm SD) before stimulation to 3.45 ± 3.54 Hz during stimulation ($n = 44$ units from 5 mice; $p = 1.07 \times 10^{-8}$, Wilcoxon signed rank test, Fig. 2A,B). When tested on a unit-by-unit basis 20 of the 44 recorded units showed a significant reduction in firing activity while none showed a significant increase (Fig. 2B, left). The median reduction in spike rate across these cells was 1.78 ± 1.36 Hz. Across the population of all recorded units, the decrease in spontaneous firing rate persisted for the duration of the 10 s optical stimulation (Fig. 2B, right). Following the stimulation, an increase in spiking was observed that returned to prestimulation levels within 20 s after stimulation ceased. Since population time course onsets appeared different for GABAergic and cholinergic modulation of spontaneous MTC firing we calculated onset times and found that cholinergic fiber stimulation derived effects were indeed significantly slower compared to GABAergic fiber derived effects (GAD-Cre 0.29 ± 0.27 s vs. ChAT-Cre 1.33 ± 1.43 s, $p = 9.19 \times 10^{-5}$, Mann–Whitney U test).

Thus, optogenetic activation of GABAergic BF fibers at the level of the OB leads to a fast reduction of MTC spontaneous activity while activating cholinergic fibers causes output neuron excitation in a slower manner, demonstrating that these subpopulations exert opposing effects with distinct time courses on spontaneous MTC firing.

To rule out optical activation artifacts, we stimulated the OB of uninjected control mice with the same parameters as before during the no sniff condition since in this condition even small changes could have been detected (Supp. Fig. 2). We found that optical stimulation led to no significant change in spontaneous firing rate ($n = 19$ units from three mice; 6.10 ± 4.15 Hz before stimulation, 6.20 ± 4.25 Hz during stimulation (mean \pm SD); $p = 0.365$, Wilcoxon signed rank test). Thus, the light-evoked modulation of spontaneous MTC firing in Chr2-injected ChAT-Cre and GAD-Cre mice was attributable to cholinergic/GABAergic signaling mediated by the optogenetic activation of cholinergic/GABAergic axons in the OB.

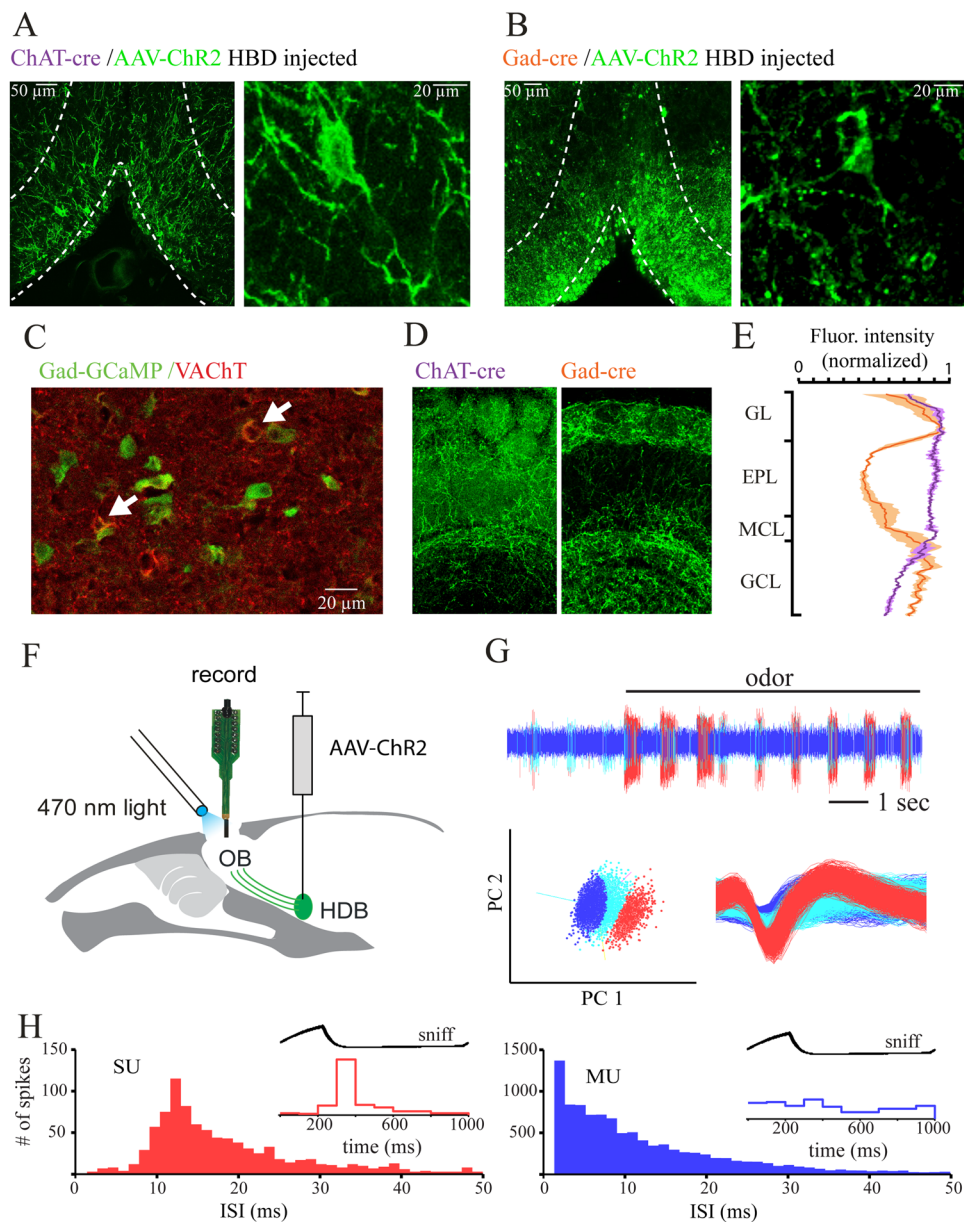


Figure 1. Selective targeting of cholinergic and GABAergic inputs from basal forebrain to the OB. **(A)** Left, Coronal section (Bregma 0.74) through BF in a ChAT-Cre mouse injected with a Cre-dependent AAV-ChR2 virus. White lines indicate the outline of HDB and VDB. Right, Magnification of HDB showing labeled ChAT+ neurons. **(B)** Left, Coronal section (Bregma 0.74) through BF in a GAD2-Cre mouse injected with a Cre-dependent AAV-ChR2 virus. White lines indicate the outline of HDB and VDB. Right, Magnification of HDB/VDB showing somata of GAD+ neurons. **(C)** Immunohistochemical staining of coronal sections of GAD2-Cre:GCaMP6 reporter mice (Bregma 0.74). Double labeled neurons are marked with white arrows. **(D)** Chr2-EYFP-expressing axon terminals in different layers of the OB 4 weeks after AAV-ChR2-EYFP injection into BF of a ChAT-Cre and Gad-Cre mice. GL: glomerular layer, EPL: external plexiform layer, MCL: mitral cell layer, GCL: granule cell layer. **(E)** Normalized fluorescence intensity profiles show that axons reaching the external plexiform layer are less prominent in Gad-Cre mice. **(F)** Schematic of experimental approach. See Materials and Methods for details. **(G)** Data acquisition. In continuous recordings, action potential waveforms with a signal-to-noise ratio of at least 4 SD above baseline noise were saved to a disk (sample rate 24 kHz) and further isolated using off-line spike sorting. The vertical line indicates onset of odorant stimulation. Isolation of waveforms into three different units by principal components 1 and 2 (bottom, left). Spike waveforms of the isolated units (bottom, right). **(H)** Inter-spoke-interval histograms for two units. One is a single unit (SU) and one a multi unit (MU). Only single units were analyzed further. For units to be classified as presumptive MTCs also a clear sniff-modulation in sniff-triggered spike averages had to be present (inset).

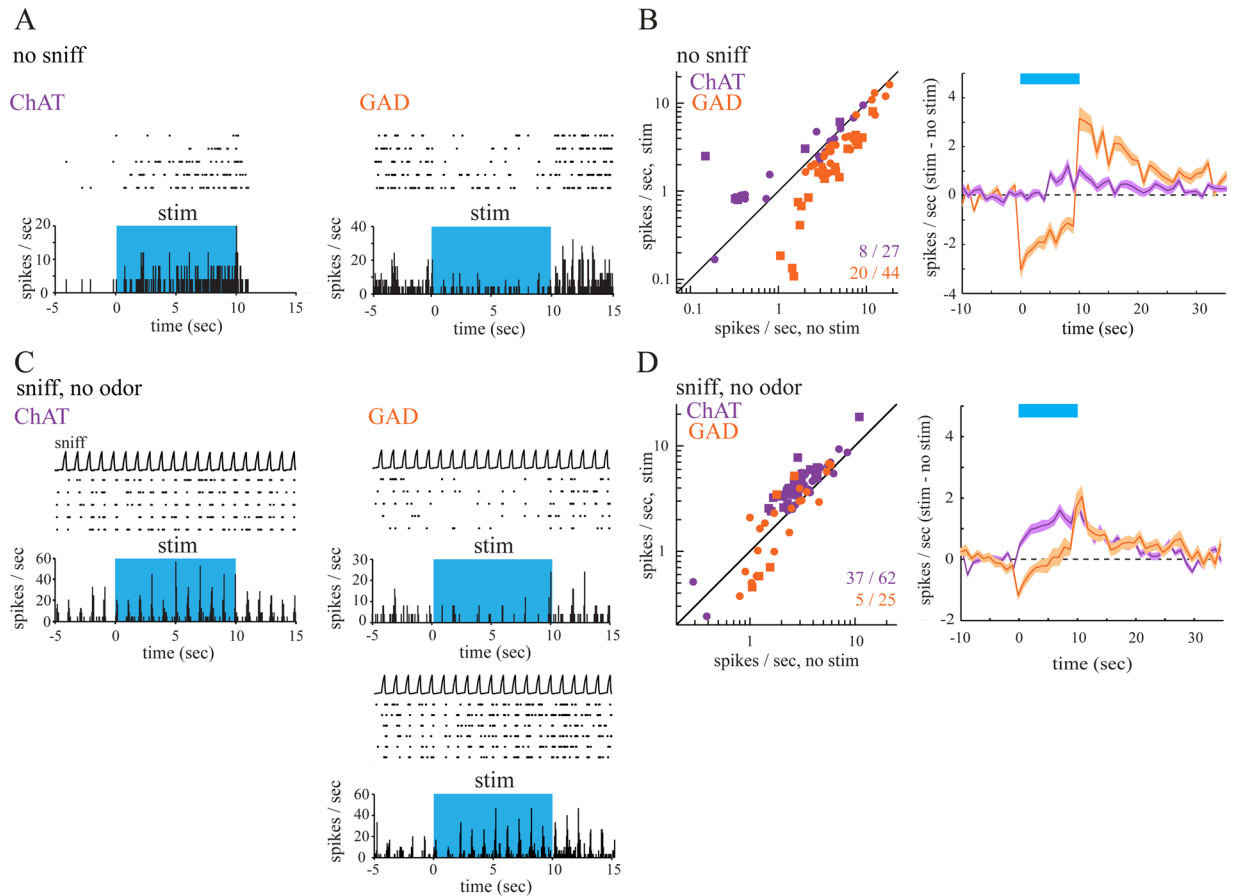


Figure 2. Optogenetic activation of cholinergic and GABAergic basal forebrain inputs to the OB modulates spontaneous as well as sensory-evoked MTC spiking. **(A)** Spike raster and rate histograms (bin width, 50 ms) from presumptive MTCs showing spontaneous spiking in the absence of inhalation (no sniff). Spike rate decreased during optical stimulation of the dorsal OB (“stim”, blue shaded area) in GAD-Cre mice and increased in ChAT-Cre animals. **(B)** Left, Plot of spontaneous firing rate in the 9 s before (no stim) and during (stim) optical stimulation for all tested units (ChAT-Cre, $n = 27$ units, purple; GAD-Cre, $n = 44$ units, orange). Squares indicated significantly modulated units. Right, Time course of changes in firing rate (mean \pm SEM across all units) during optical stimulation (blue bar). The trace indicates changes in mean spike rate in 1 s bins relative to the mean rate before stimulation. The time axis is relative to the time of stimulation onset. **(C)** Spike raster and rate histogram of MTC spiking during inhalation of clean air and optical stimulation (blue shaded area). Inhalation-evoked spike rates decrease (top) or increase (bottom) during optical stimulation in GAD-Cre mice while only excitation in response to optical stimulation is observed in ChAT-Cre mice. The top trace (sniff) shows artificial inhalation as measured by a pressure sensor connected to the nasopharyngeal cannula. **(D)** Left, Plot of inhalation-evoked firing rates during clean air inhalation, averaged for the nine inhalations just before (no stim) and after (stim) optical stimulation (ChAT-Cre, $n = 62$ units, purple; GAD-Cre, $n = 25$ units, orange). Data were analyzed and plotted as in B. Squares indicate significantly modulated units. Right: Time course of changes in firing rate (mean \pm SEM across all units) during optical stimulation (blue bar).

Optogenetic activation of cholinergic and GABAergic axons in the OB modulates inhalation-evoked MTC spiking.

Next, we investigated the effect of cholinergic and GABAergic axon activation on MTC responses during artificial inhalation of clean air (Fig. 2C,D). Inhalation-linked spiking patterns could be observed in 62 units (4 mice) in ChAT-Cre and 25 units (6 mice) in GAD-Cre mice, most likely reflecting weak sensory-evoked responses^{28,59,60}.

Optical stimulation of cholinergic axons in ChAT-Cre mice significantly increased inhalation-linked spiking of MTCs (Fig. 2C), with the median spike rate increasing from 2.86 ± 1.72 Hz to 4.03 ± 2.45 Hz during optical stimulation ($p = 2.99 \times 10^{-11}$, Wilcoxon signed rank test). When tested on a unit-by-unit basis, 37 of 62 recorded units (60%) showed a significant optical stimulation evoked increase in spiking (Fig. 2D); none showed a decrease. Inhalation evoked spiking of these 37 cells increased by 1.33 ± 1.29 spikes/sniff/s.

In GAD2-Cre mice, optical stimulation led to mixed effects on inhalation-linked spiking that were not significant across the population of MTCs (1.8 ± 1.66 Hz before stimulation, 2.26 ± 2.13 Hz during stimulation; $n = 25$ units from 6 mice; $p = 0.58$ Wilcoxon signed rank test, Fig. 2C,D). When tested on a unit-by-unit basis three of the 25 (12%) units showed a significant decrease and two (8%) a significant increase in firing activity. Inhalation evoked spiking decreased by 0.67 ± 0.14 spikes/ sniff/s and increased by 2.35 ± 0.71 spikes/ sniff/s for

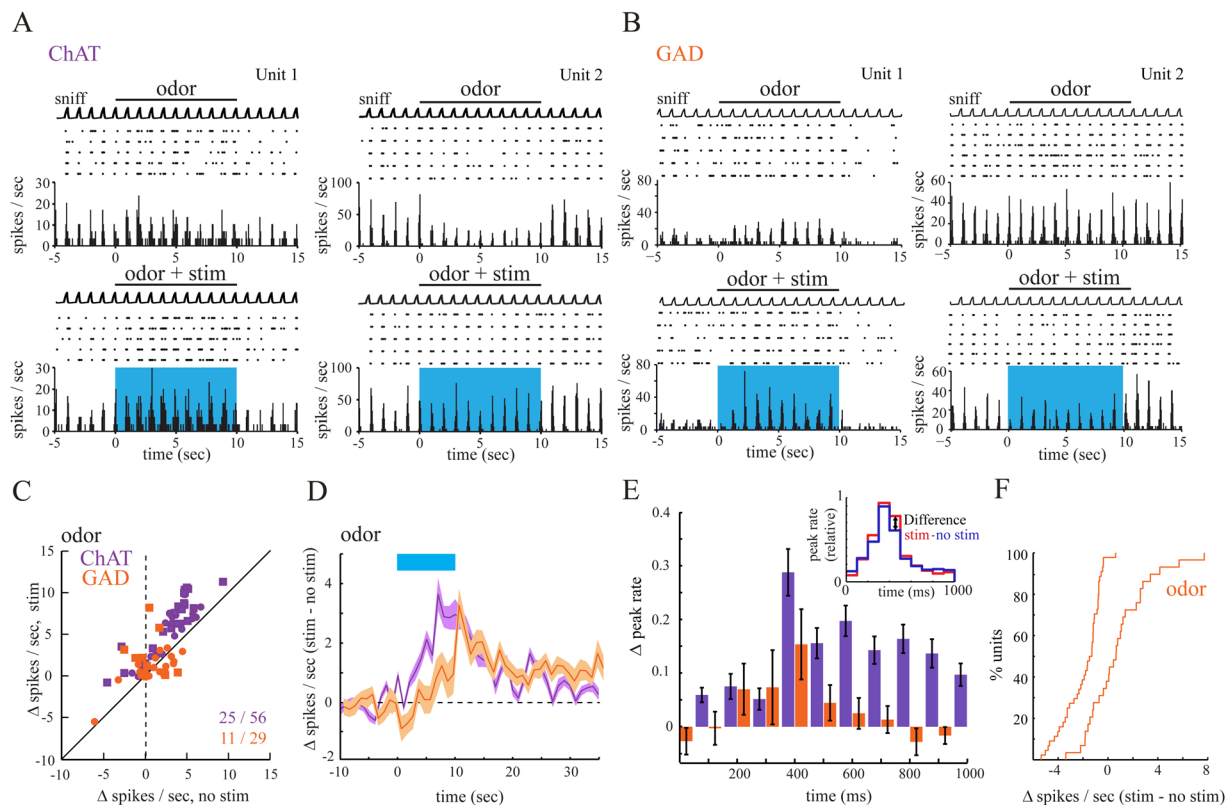


Figure 3. Optogenetic activation of cholinergic and GABAergic OB inputs modulates odor-evoked responses. **(A)** Odorant-evoked MTC spiking is enhanced by optical OB stimulation in ChAT-Cre mice in both odorant-activated (Unit1) and odorant-inhibited (Unit2) cells. **(B)** Odorant-evoked MTC spiking is increased (left) or decreased (right) by optical OB stimulation in GAD-Cre mice. **(C)** Plot of odorant-evoked changes in MTC spiking (Δ spikes/sniff) in the absence of (no stim) and during (stim) optogenetic stimulation of cholinergic ($n = 56$ units, purple) or GABAergic ($n = 29$, orange) afferents to the OB. **(D)** Time course of effects of optical stimulation on odorant-evoked spike rate, averaged across all units. The blue bar shows time of optical stimulation and simultaneous odorant presentation. Plotted is the mean change in odorant-evoked spike rate between trials with and without light stimulation, measured after each inhalation (at 1 Hz); the shaded area indicates variance (SEM) around mean. **(E)** Optical stimulation induced firing changes during the sniff cycle. Cholinergic modulation increased the firing rate across the sniff cycle. GABAergic modulation increased firing in peak and adjacent time bins while inhibiting firing outside the “preferred sniff phase”. Firing changes were calculated from sniff-triggered spike histograms as depicted in the inset. **(F)** Cumulative probability plots comparing changes in MTC firing rates caused by optical stimulation in the no sniff and odor condition. Plots reflect datasets plotted in Figs. 2B and 3C, respectively. Unlike the uniform suppression of spontaneous spiking observed in GAD-Cre mice, optical stimulation in the odor condition predominantly causes MTC excitation.

the significantly inhibited and excited units, respectively. The averaged time course depicted an initial decrease in MTC firing rate that, in contrast to the time course in the no sniff condition, returned to prestimulation levels already during the stimulation period (Fig. 2D). Following stimulation, spike rate increased above baseline levels for approx. 20 s before returning to baseline. Taken together, while optogenetic stimulation of cholinergic fibers in both conditions was qualitatively similar, activating GABAergic fibers leads to mixed effects of MTC spiking in the sniff condition that was not observed during spontaneous spiking.

Optogenetic activation of cholinergic and GABAergic axons in the OB enhances odorant-evoked MTC spiking. Since optical activation of BF inputs to the bulb modulates inhalation-linked MTC spiking consistent with modulating weak sensory-evoked responses, we next evaluated the impact of bulbar cholinergic and GABAergic modulation on odorant responses. We compared MTC responses to odorant stimulation applied with and without optogenetic activation of cholinergic or GABAergic BF axons (Fig. 3A,B). In line with the findings from the previously tested conditions light activation of cholinergic fibers in ChAT-Cre mice increased MTC spiking (Fig. 3A,C). Across the population of recorded presumptive MTCs ($n = 56$ units, 5 mice), BF axon stimulation significantly increased MTC odor activity, with an increase from 6.49 ± 3.47 spikes/sniff/s (median \pm SD) during odorant presentation alone to 8.98 ± 4.22 spikes/sniff/s during odorant paired with light ($p = 3.93 \times 10^{-10}$, Wilcoxon signed rank test). 25 out of the 56 recorded cells (45%) showed a significant increase in odor-evoked spiking when tested on a unit-by-unit basis; none showed a decrease (Fig. 3C).

Optogenetic activation of GABAergic fibers in the OB during odor presentation elicited heterogeneous effects that, across the population of recorded cells ($n = 29$ units, 4 mice), were not significant (5.44 ± 3.12 spikes/sniff/s during odorant presentation alone, 4.93 ± 4.30 spikes/sniff/s during odorant paired with light, $p = 0.52$, Wilcoxon signed rank test). However, tested on a unit-by-unit basis eight out of 29 recorded cells (28%) showed a significant increase and three (10%) a significant decrease in odor-evoked firing activity (Fig. 3C). The modulation in spike rate across the cells showing a significant increase/decrease was $2.17/2.48$ spikes/sniff/s (from 7.53 ± 4.1 to 9.7 ± 5.32 /from 5.44 ± 0.57 to 2.96 ± 0.39), respectively. The averaged activity time course of the recorded units displayed an initial brief reduction of firing rate that switched to excitation during the stimulation period (Fig. 3D).

We also examined optical stimulation-induced changes in odor-evoked MTC spiking pattern by generating sniff-triggered spike histograms aligned to the start of inhalation for ChAT-cre and GAD-cre mice (Fig. 3E inset, see²⁸). Neither cholinergic nor GABAergic basal forebrain derived modulation showed a significant change of the time bin of peak firing across the population of recorded units ($p = 0.63$ and 1 for ChAT-cre and GAD-cre mice, respectively, paired t test). However, comparing the optical stimulation-induced firing change per bin revealed a profound difference between cholinergic and GABAergic modulation (Fig. 3E): while cholinergic modulation increased the firing rate across the sniff cycle, GABAergic modulation increased firing in peak and adjacent time bins while inhibiting firing outside the “preferred sniff phase”.

The BF receives input from different olfactory areas⁴⁵ and it has been shown that even during sleep and anesthesia, cholinergic and GABAergic BF neurons are rhythmically discharging^{61–64}. We therefore tested the effect of inhibiting cholinergic and GABAergic BF projections to the OB using the light-gated chloride pump Halorhodopsin as an optogenetic silencer (Supp. Fig. 3). Despite robust, yet sparser expression of Halo-YFP, labeling could be observed in the OB for both ChAT-Cre and GAD-Cre mice four weeks after viral injection (Supp. Fig. 3A). Optogenetic stimulation during recording of presumptive MTCs (Supp. Fig. 3B) showed, when tested on a unit-by-unit basis, no significant effects in ChAT-Cre animals (8 units, 2 mice) while only two out of 28 recorded cells showed a weak but significant decrease in odor-evoked spiking (0.47 spikes/sniff/s) in GAD-Cre animals (Supp. Fig. 3C). No significant modulation effects were observed in the other tested conditions (no sniff and sniff, data not shown). This was also true for units showing strong sensory-evoked spiking, rendering it unlikely that effects went undetected due to low spike counts. The surprisingly weak effects of optogenetic inhibition might be the result of only weak spontaneous cholinergic and GABAergic HDB activity in the anesthetized animal.

In uninjected control mice (Supp. Fig. 2), the same optical stimulation led to no significant change in spontaneous firing rate ($n = 11$ units from three mice; 6.31 ± 5.56 Hz before stimulation, 6.26 ± 5.47 Hz during stimulation (mean \pm SD); $p = 0.61$, Wilcoxon signed rank test).

GABAergic modulation of OB output is sensory input dependent. Unlike spontaneous spiking, which got suppressed by optical stimulation in GAD-Cre mice, the same optical stimulation during odor stimulation predominantly caused MTC excitation (Fig. 3F). In a separate set of experiments, we therefore investigated if this suppression to excitation transition can also be observed on a single unit basis, or might be caused by a recording bias e.g. through different populations of output neurons being detectable in the different conditions. We recorded GABAergic modulation effects in individual MTC tested in both the spontaneous as well as the odorant evoked condition in one continuous session (Fig. 4A,B depict recordings from the same unit).

As shown previously (Fig. 2), optical stimulation in the no sniff condition led to a significant reduction in MTC spontaneous spiking across all recorded units (3.61 ± 3.43 Hz before stimulation; 3.14 ± 3.37 Hz during stimulation; $n = 53$ units from 3 mice; $p = 0.014$ Wilcoxon signed rank test). When tested on a unit-by-unit basis 5 of the 53 units recorded showed a significant reduction in firing activity and only two units showed an increase (Fig. 4C). Similar to the previous findings (Fig. 3), GABAergic axon activation during odor presentation had a predominantly excitatory effect on MTC activity (7.35 ± 8.12 spikes/sniff/s during odorant presentation alone, 8.13 ± 9.47 spikes/sniff/s during odorant paired with light, $p = 9.86 \times 10^{-10}$, Wilcoxon signed rank test). Moreover, all significantly modulated units (22 out of 53 cells (42%)) showed an optical stimulation-induced increase in odor-evoked spiking, none showed a decrease. Quantitative comparison of the optogenetic stimulation effect in both conditions showed a significantly more positive modulation in the odor compared to the spontaneous condition (Fig. 4E; spontaneous spiking -0.31 ± 1.61 vs. odor-evoked spiking 1.98 ± 2.01 (median \pm SD); measured as Δ spikes/s relative to non-stimulation condition; $p = 6.34 \times 10^{-9}$, Wilcoxon signed rank test). Comparing the firing rate of individual units between the conditions revealed that almost all recorded units (48 of 53 units) showed a more positive, optically evoked modulation in spike rate in the odor compared to the no sniff condition.

To investigate whether the observed modulation was dependent on baseline firing rates we plotted the optical stimulation effect as a function of baseline activity. As expected, baseline firing activity was lower in the no-sniff compared to the odor condition (3.61 ± 3.43 (median \pm SD) spikes/sec compared to 7.35 ± 8.11 spikes/sec; $p = 2.53 \times 10^{-6}$, Wilcoxon signed rank test). Interestingly, while optical stimulation effects in the odor condition were positively correlated to baseline activity (Pearson's $r = 0.61$; two-tailed, $p = 1.47 \times 10^{-6}$) a negative correlation was observed in the no-sniff condition (Pearson's $r = -0.27$; two-tailed, $p = 0.05$). These results suggest that the stimulation effect most likely depends on the amount of sensory input rather than solely on the absolute firing rate prior to optical stimulation. The results furthermore indicate that the inhibition to excitation transition across conditions can also be observed on a single unit basis and thus that GABAergic fiber derived modulation can act in a bimodal way on single OB output neurons.

Previous studies have suggested a sharpening of MTC odorant responses by cholinergic modulation through preferentially suppressing weak MTC responses and enhancing inhibitory responses^{27,33,43}. Since we only observed additive cholinergic modulation effects on MTC activity, suggesting no change of tuning in accordance with a previous report²⁸, we asked if the GABAergic basal forebrain subsystem might be capable of sharpening odor responses in the OB. In a separate set of experiments (36 units, from 3 animals), we therefore tested the response

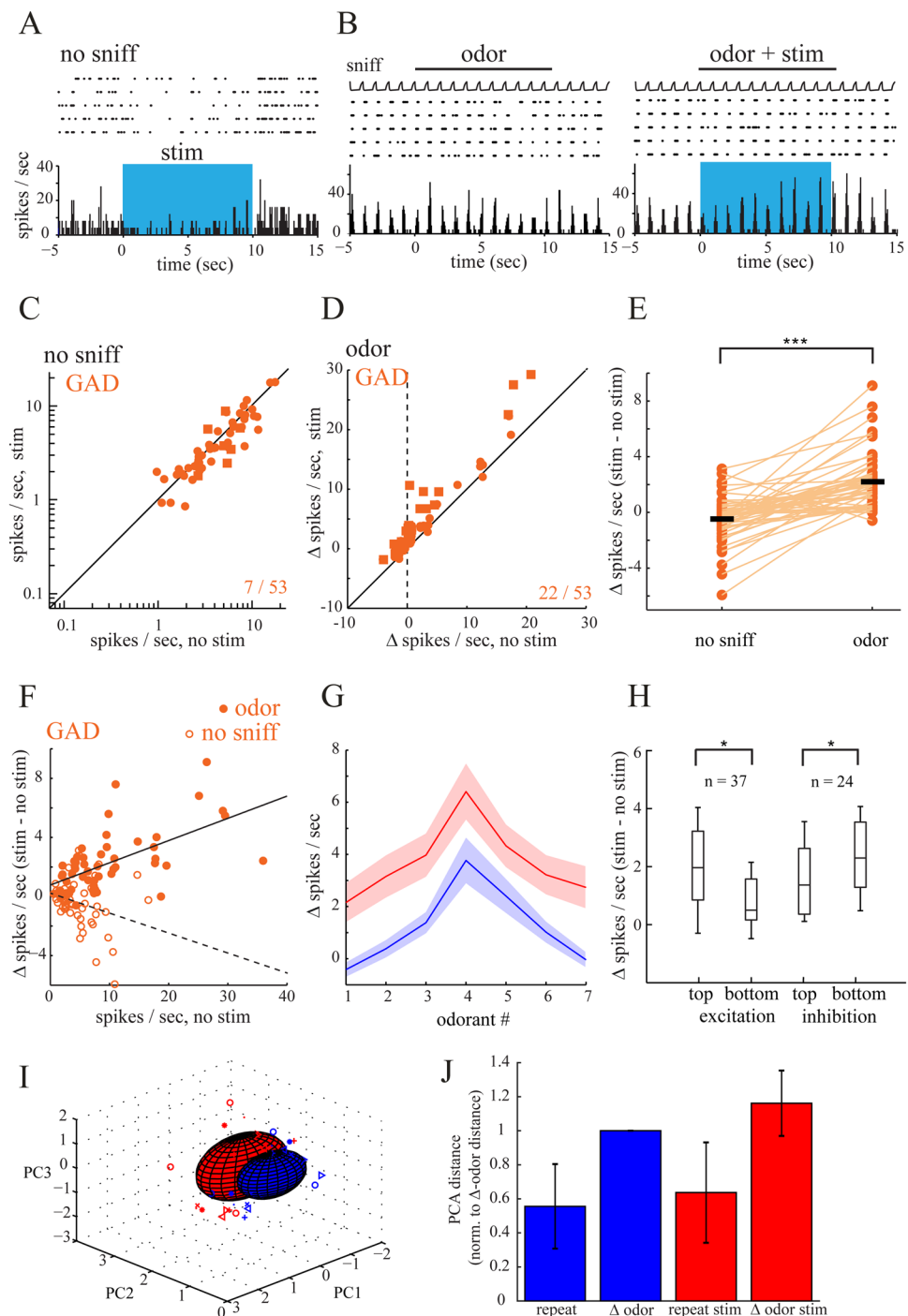


Figure 4. Switch in modulatory effect between conditions in GAD-Cre mice. **(A)** Spike raster and rate histogram (bin width, 50 ms) depicting a spike rate decrease for a MTC during optical stimulation of the dorsal OB (“stim”, blue shaded area). **(B)** The same unit plotted in **A** was also tested in the odor condition. Odorant-evoked spiking is enhanced by optical stimulation in this unit. **(C)** Plot of spontaneous firing rate in the 9 s before (no stim) and during (stim) optical stimulation for all units tested in both the no-sniff and the odor condition ($n = 53$ units). Squares indicated significantly modulated units. **(D)** Plot of odorant-evoked spiking changes (Δ spikes/sniff) in the absence of (no stim) and during (stim) optogenetic stimulation of the same units tested in **C**. **(E)** Quantitative comparison of stimulation-evoked spiking changes (Δ spikes/sec) in the no-sniff and odor condition. Circles, spiking changes for individual units; black bars, mean value. Lines connect the same unit across conditions. **(F)** Optical stimulation effects in the odor condition were positively correlated to baseline activity (Pearson’s $r = 0.61$; two-tailed, $p = 1.47 \times 10^{-6}$). A negative correlation was observed in the no-sniff condition (Pearson’s $r = -0.27$; two-tailed, $p = 0.05$). **(G)** Effect of optical GABAergic OB fiber stimulation on odorant responses for MTCs tested with seven odorants. Blue, baseline response; red, response during optical stimulation. Odorants are ordered separately for each unit, with the strongest excitatory response in the baseline condition in the middle of the abscissa. Lines (\pm SEM) connect median responses across all tested

trials. (H) Box plot comparing optically induced change in odorant-evoked spike rate (stim - no stim) for the strongest and weakest quartile of odorant-evoked responses taken from all cell-odorant pairs for excitatory as well as inhibitory responses. The box indicates median, 25–75th percentile ranges of the data, and whiskers indicate ± 1 SD from the mean. (I) Representative PCA representation of OB response to odors with (red) and without (blue) OB HDB fiber activation. Symbols represent responses on individual trials to each odorant; ellipsoids are mean ± 1 SD. (J) Relative population response distances in neural activity space projected onto the first three principal components. Distances were normalized to the average Δ odor distance. OB GABAergic fiber activation increases both variability in repeat and Δ odor responses.

of the same MTC to multiple odorants with and without optical GABAergic OB fiber stimulation. Consistent with our previous findings, we found that odorant responses were mostly enhanced (0.39 ± 3.22 spikes/sniff/s during odorant presentation alone, 2.41 ± 5.01 spikes/sniff/s during odorant paired with light, $p = 1.79 \times 10^{-40}$, Wilcoxon signed rank test). Stimulation effects on tuning curves varied between units. An average tuning curve, calculated across the population of all recorded units (Fig. 4G) displayed a uniform, odor strength independent increase in firing rather than a change in tuning. However, when odorant-cell responses were collapsed across units creating a large dataset of 252 cell odor pairs (Fig. 4H), a comparison of the optically induced change in odorant-evoked spike rate (stim - no stim) for the strongest and weakest quartile of odorant-evoked responses revealed weak but significant differences for excitatory (unpaired Wilcoxon rank-sum test, $p = 0.03$; $n = 37$ cell-odor pairs) as well as inhibitory (unpaired Wilcoxon rank-sum test, $p = 0.01$; $n = 24$ cell-odor pairs) responses. These results might point to strong odorant responses receiving more excitatory modulation from GABAergic basal forebrain derived fibers no matter if their particular odorant response is excitatory or inhibitory. Based on this result we asked whether MTC responses to different odorants become more dissimilar with optogenetic stimulation of GABAergic fibers, potentially enhancing odor classification in the respective cells.

We therefore characterized the OB HDB stimulation effect by constructing trial-by-trial response vectors composed of spike counts for each cell and projected these high-dimensional responses onto their three principal components (Fig. 4I). We quantified the variance for repeated odor presentations of each odor (repeat) and responses to different odors (Δ odor), with and without stimulation (Fig. 4J). OB HDB fiber activation led to an increased Euclidian distance in repeat and Δ odor responses pointing to more dissimilar odor responses, potentially supporting enhanced odor classification.

Discussion

The basal forebrain is critical for many cognitive processes^{65–69} as well as for sensory information processing^{51,70–75}. Despite longstanding knowledge about the heterogeneity of BF derived long-range projections^{17,25,76,77}, studies examining their function in sensory processing so far have been focused almost exclusively on cholinergic projections^{3,27,28,46,78–82}.

Here, we examine the effect of GABAergic long-range projections in the olfactory bulb (OB) and provide for the first time a direct comparison of cholinergic and GABAergic modulation effects on early sensory processing under the same experimental conditions.

Expression and activation of channelrhodopsin in basal forebrain projections. Differential expression of channelrhodopsin in either GABAergic or cholinergic long-range projections was achieved by injection of AAV-ChR2 into the BF of GAD2 or ChAT-cre mice, respectively. Expression patterns showed a relatively homogenous distribution of cholinergic fibers in the OB in accordance with previous publications. Distribution of GABAergic fibers only differed slightly from a previous publication that used the same transgenic mouse line with a similar expression strategy⁴⁷. Similar to their results we saw dense labeling in the granule cell layer, but equally strongly labeled glomerular layer and a slightly weaker labeled mitral cell layer. This slight difference could be the result of viral injection sites since Nunez-Parra *et al.* targeted more posterior parts of BF.

A recent report points to a potential coexpression of cholinergic and GABAergic markers at the level of the OB⁸³. Different from this study we found that less than 10% of GAD expressing cells were also positive for a cholinergic marker. In combination with the distinct cholinergic and GABAergic expression patterns and photostimulation effects observed here, our findings suggest that these projections are mainly separated and ACh and GABA are most likely not being predominantly released from the same fibers.

Activation of long-range projections was performed by photostimulating axonal fibers at the dorsal surface of the OB. While known to be less effective compared to somatic stimulation⁸⁴, optogenetic fiber stimulation at the level of the OB was necessary to obviate potential indirect BF modulation effects of OB activity: First, optogenetically activating BF might cause a stimulation of brain areas also targeted by BF fibers that in turn project to the OB^{25,76,77,85–91}. Second, a direct BF stimulation in GAD-Cre mice would cause activation of a large amount of GAD positive inhibitory BF interneurons^{92,93}. Third, cholinergic BF neurons were shown to excite GABAergic projection neurons^{94–96}, thereby also rendering a direct BF stimulation problematic. Axonal fibers at the dorsal surface of the OB were activated using a continuous stimulation paradigm, which has been shown to be most effective in activating cholinergic axonal fibers^{28,97}. BF fiber silencing with inhibitory opsins hardly showed any MTC activity modulation in the different conditions (sniff, no sniff, odor). The surprisingly weak effects of optogenetic inhibition might be the result of only weak spontaneous cholinergic and GABAergic HDB activity in the anesthetized animal.

Effects of basal forebrain projections on OB output cell activity. Recording from olfactory bulb output neurons, we show that, in contrast to a local and specific activation of cholinergic fibers, that add an excitatory bias to mitral/tufted cell firing, a selective activation of GABAergic BF fibers leads to bimodal, sensory

input dependent effect on OB output: whereas optogenetic stimulation mainly inhibited spontaneous MTC firing, odor-evoked MTC cell spiking was predominantly enhanced; an effect that could also be observed on a single neuron level. Though we cannot exclude that the subpopulation of GABAergic cells showing cholinergic markers is partially or completely overlapping with GABAergic bulbopetal neurons in the HDB, this strong functional divergence, renders this possibility, in our opinion, unlikely.

Onset time, at least for modulation of spontaneous firing was slower for cholinergic modulation compared to GABAergic modulation. This is in agreement with a previous publication using that same stimulation technique, showing that cholinergic effects of spontaneous activity appear slower compared to modulations on sensory-evoked activity (28 Fig. 3H). The underlying causes of this slow onset remain to be elucidated, but it might be that in the absence of sensory input the effect of “direct” cholinergic MTC modulation is especially prominent. So far there are no reports demonstrating synaptic contacts of cholinergic fibers with MTCs, despite the presence of nAChRs on MTCs⁹⁸. Thus, at least part of cholinergic transmission could happen extrasynaptically, a process that operates on a slower time scale than synaptic transmission⁹⁹.

Additionally, MTCs showed a reduction of firing outside and an increase of firing within the preferred sniff phase. This modulation is strongly reminiscent of a model of a bimodal gain change evoked by attention⁹ also referred to as filtering. These filter processes are reported to dampen activity to non-attended or background stimuli while enhancing relevant sensory input. Indeed, in the odor condition, the size of the GABAergic modulation effect was dependent on the odor-evoked firing activity for both excitatory and inhibitory odor responses, pointing to a multiplicative population firing change for relevant olfactory stimuli while decreasing background activity. Additionally, our data seem to show that odor responses within cells become more dissimilar with GABAergic fiber stimulation, raising the possibility of enhancing odor classification of MTCs.

Our direct comparison of cholinergic and GABAergic OB fiber activation suggest that both BF derived fiber systems might have a role in gain modulation of OB output, but in a very distinct way: while cholinergic modulation seems to act in a fashion rather similar to baseline control⁴⁶, GABAergic modulation seems to lead to a filtering of weak signals in the OB.

Possible circuit mechanisms underlying bulbar GABAergic modulation. The circuit mechanisms underlying basal forebrain derived modulation effects remain to be elucidated since a comprehensive list of targets for BF fibers in the OB is missing especially for GABAergic projections. Cholinergic and GABAergic systems most likely exert multiple effects within the OB with different receptors, cell types, and modes of transmission (volume vs. strict synaptic transmission) involved⁹⁸.

Though cholinergic modulation of OB circuits has been described in numerous publications (see for review⁹⁸), the circuit mechanisms underlying this modulation are quite complex and not yet described in their entirety. Cholinergic fibers from the HDB project to all layers of the OB^{28,55,56} and there is evidence for the presence of both nicotinic (nAChRs^{100,101}), as well as muscarinic ACh receptors^{29,102} within the OB. It is so far unknown how the different players of cholinergic modulation in the OB interact to create an effect on olfactory bulb output. The here described excitatory effect on MTCs is in agreement with a previous publication²⁸ and might be derived from activation of nAChRs on mitral cells and/or external tufted cells which provide MTC feed-forward excitation^{103–105}.

Just like in several other brain areas¹⁰⁶, GABAergic BF axons in the OB are so far only reported to synapse on inhibitory interneurons^{23,47}; centrifugal GABAergic afferents were shown to inhibit granule cells⁴⁷ deep short axon cells^{48,83} as well as different types of periglomerular cells⁴⁸. Inhibition of those inhibitory interneuron subtypes would, in the simplest case, result in a disinhibition of mitral and tufted cells and could explain the here observed MTC excitation. The sensory input dependent increase in excitatory modulation between conditions and the correlation of effects size with odorant evoked responses could be the result of an increase in sensory dependent activity in OB interneurons¹⁰⁷ leading to a further increase in disinhibition (Suppl. Fig. 4). The observed inhibition in MTCs could be elicited by a multisynaptic effect via several types of inhibitory interneurons: neurons like deep short axon cells and PG cells (which receive GABAergic BF input⁴⁸) were shown to inhibit other inhibitory interneurons like periglomerular and granule cells, respectively (see¹⁰⁸). However, the fast, strong, and persistent nature of this inhibition, rather argues for a direct inhibitory input to MTCs (Suppl. Fig. 4) similar to that observed in the basolateral amygdala where BF GABAergic fibers provide indirect disinhibition, as well as direct inhibition of pyramidal neurons¹⁰⁹. Since recording interneuron activity in the OB in anesthetized animals is challenging due to their diminished activity^{110–112}, future experiments in awake animals will test the relative contribution of different types of neurons on the observed effects.

It will be interesting to see how the, here described, dual modulation effect of GABAergic basal forebrain fibers translates to olfactory sensory responses in the awake animal. During wakefulness, the proposed direct inhibitory effect on MTCs could be diminished due to the sparsening of MTC responses¹¹⁰ or contribute itself to sparser MTC responses. At the same time, the excitatory effect via inhibitory interneurons might be vastly increased due to the increased activity in those neurons¹¹¹. In general, while it is hard to estimate the net modulation effect, it is likely that the increase in interneuron and basal forebrain neuron activity in awake animals^{64,113} will lead to a stronger effect of BF modulation in this condition.

Conclusion

Our recordings provide, for the first time, a detailed comparison of BF cholinergic and GABAergic influence on early sensory processing and highlight the potential of the noncholinergic BF population to modulate perception. By inhibiting weak and facilitating strong inputs, GABAergic BF fibers in the OB likely increase MTCs signal-to-noise ratio, a hallmark of attentional processes that have been previously attributed mainly to cholinergic processes^{2–4,9,10}. Our findings are in line with recent data indicating that the classical view on the (cholinergic) BF system might be oversimplified: activity of non-cholinergic BF neurons was more strongly correlated

with arousal and attention^{11–15}, whereas cholinergic neuron activity was correlated with body movements, pupil dilations, licking, punishment^{75,114} as well as primary reinforcers and outcome expectations¹¹. The distinct early sensory modulation effects of cholinergic and GABAergic BF neurons observed in this study might therefore be owed to the different functions of these two basal forebrain systems. Here we targeted cholinergic and GABAergic projections neurons located primarily in the same area (HDB) since previous publications have shown that populations from different basal forebrain centers can have heterogeneous effects⁸¹. However, we cannot exclude that the effects observed during GABAergic fiber stimulation were, at least partially, derived from GABAergic fibers originating in the MCPO, a nucleus containing a majority of GABAergic bulbopetal neurons^{23,25,47,115}. Future studies, examining the influence of GABAergic projections from different basal forebrain centers will hopefully be able to clarify this issue. Addressing the exact interplay between ACh and GABA in olfactory bulb sensory processing in the awake animal will be critical to fully understand the relative contribution of each system.

Materials and Methods

Animal strains and care. We used mice expressing Cre recombinase under control of the choline acetyltransferase (ChAT-Cre mice; JAX Stock #006410, The Jackson Laboratory) or glutamate decarboxylase 2 (GAD2-Cre mice, JAX Stock #010802, The Jackson Laboratory) promoter^{49,50}. Animals of either sex were used. Animals were housed under standard conditions in ventilated racks. Mouse colonies were bred and maintained at RWTH Aachen University animal care facilities. Food and water were available *ad libitum*. Experimental protocols were approved by the “Landesamt für Natur, Umwelt und Verbraucherschutz NRW (LANUV NRW) (State Office for Nature, Environment and Consumer Protection North Rhine-Westphalia), Postfach 10 10 52, 45610 Recklinghausen, Germany” and comply with European Union legislation and recommendations by the Federation of European Laboratory Animal Science.

Viral vectors. Viral vectors were obtained from the viral vector core of the University of Pennsylvania or Addgene. Vectors were from stock batches available for general distribution. pAAV-EF1a-double floxed-hChR2(H134R)-EYFP-WPRE-HGHpA and pAAV-Ef1a-DIO eNpHR 3.0-EYFP were a gift from Karl Deisseroth (Addgene viral prep # 20298-AAV1; <http://n2t.net/addgene:20298>; RRID: Addgene_20298 and Addgene viral prep # 26966-AAV1; <http://n2t.net/addgene:26966>; RRID: Addgene_26966). Injection of Cre-dependent vector (AAV1.EF1a.DIO.hChR2(H134R)-eYFP.WPRE.hGH (AAV.FLEX.ChR2.YFP) and AAV1.EF1a.DIO.eNpHR3.0-eYFP.WPRE.hGH (AAV.FLEX.HR.YFP)) was performed as described in^{28,111}. Briefly, BF virus injection (relative to Bregma (in mm) +0.74 anteroposterior, 0.65 mediolateral, –4.8 dorsoventral,¹¹⁶). Virus (0.5–0.75 μ l; titer 1.97×10^{12} – 2.35×10^{12}) was delivered through a 26 gauge metal needle at a rate of 0.1 μ l/min. Mice were individually housed for at least 28 days before being evaluated for transgene expression or recording.

Olfactometry. Odorants were presented as dilutions from saturated vapor in cleaned, humidified air using a custom olfactometer under computer control^{28,117,118}. Odorants were typically presented for 10 seconds. All odorants were obtained at 95–99% purity from Sigma-Aldrich and stored under nitrogen/argon. The following odorants were used: ethyl butyrate, 2-hexanone, methyl valerate, valeraldehyde, methyl hexanoate, isoamyl acetate, sec-butyl acetate, vinyl butyrate, and ethyl tiglate. Odorants were presented at 1% saturated vapor (s.v.).

Extracellular recordings and optical stimulation. MTC unit recordings and optical OB stimulation were performed as described previously²⁸ with several modifications. Briefly, mice were anesthetized with pentobarbital (50 mg/kg) and placed in a stereotaxic device. Mice were double tracheotomized and an artificial inhalation paradigm was used to control air and odorant inhalation independent of respiration^{119–121}. Extracellular recordings were obtained from OB units using sixteen channel electrodes (NeuroNexus, A1x16-5mm50-413-A16, Atlas Neuro, E16 + R-100-S1-L6 NT) and an RZ5 digital acquisition system (TDT, Tucker Davis Technologies). Recording sites were confined to the dorsal OB. Action potential waveforms with a signal-to-noise ratio of at least 4SD above baseline noise were saved to a disk and further isolated using off-line spike sorting (Open-Sorter; TDT, Fig. 1F). Sorting was done using the Bayesian or (in fewer cases) K-Means cluster cutting algorithms in OpenSorter. Units were defined as “single units” if they fell within discrete clusters in a space made up of principal components 1 and 2. Units with interspike intervals lower than the absolute refractory period (<2.5 ms) were excluded from further analysis¹²² (Fig. 1G). For units to be classified as presumptive MTCs, units additionally had to be located in the vicinity of the mitral cell layer, show spiking activity in the absence of odorants, and a clear sniff-modulation (the maximum spike rate in a 100 ms bin had to be at least two times the minimum spike rate for the PSTH (Fig. 1G insets)); similar as described in⁵⁷. Subsequent analyses were performed using custom scripts in Matlab. Odorant alone (‘baseline’) and odorant plus optical stimulation trials (at least 3 trials each) were interleaved for all odorants (inter-stimulus interval 40–50 s). Recordings were subject to unit-by-unit statistical analysis as described below.

For optical OB stimulation, light was presented as a single 10 sec pulse either alone or simultaneous with odorant presentation using a 470 or 565 nm LED and controller (LEDD1B, Thorlabs) and a 1 mm optical fiber positioned within 3 mm of the dorsal OB surface as in earlier studies²⁸. The light power at the tip of the fiber was maximal 3 and 10 mW for the 565 nm and 470 nm LED, respectively.

Extracellular Data analysis. Basic processing and analysis of extracellular data followed protocols previously described for multichannel MTC recordings²⁸. Responses to optical or odorant stimulation were analyzed differently depending on the experimental paradigm. Stimulation effects on spontaneous spike rate (no artificial inhalation, “no-sniff” condition) were measured by calculating spikes/second (Hz) for the 9 sec before or during

stimulation. Selection of ‘sniff modulated’ units was performed as described previously²⁸. Response latency was defined as the time difference between the stimulus onset and the response onset. For determining response onset we calculated the response latency of single units from averaged conditions by taking the first bin where the averaged response intersects a horizontal line indicating two standard deviations (SD) above the baseline activity within the evaluation window. The bin number was then converted to and reported in milliseconds (ms). Inhalation-evoked responses during inhalation of clean air (“sniff” condition) were measured by averaging the number of spikes per 1-sec period following each inhalation in the 9 inhalations pre-stimulation or during stimulation and across multiple trials (minimum of 3 trials in each condition for all units). Odorant-evoked responses were measured as changes in the mean number of spikes evoked per 1-sec inhalation cycle (Δ spikes/sniff) during odorant presentation, relative to the same number of inhalations just prior to odorant presentation. For statistical analysis, significance for changes in firing rate for baseline versus optical stimulation was tested on a unit-by-unit basis using the Mann-Whitney *U* test on units recorded in 5 or more trials per condition.

Principal component analysis. Principal components were computed from population response vectors using the Matlab statistical toolbox. Responses are odor presentation spike counts per trial for each cell. To compute PC distance, 3-dimensional Euclidean distances were computed for stimulation and no stimulation trials for each cell before averaging. Summary statistics were computed on these average trial-pair distances.

Statistical analysis. Significance was determined using paired Student’s *t*-test, Wilcoxon signed rank test and Mann-Whitney *U* test, where appropriate. Significance was defined as **P* < 0.05, ***P* < 0.005, ****P* < 0.0005, *****P* < 0.0001. All tests are clearly stated in the main text.

Histology and Immunohistochemistry. Viral (AAV.FLEX.ChR2.YFP, AAV.FLEX.HR.YFP) expression in BF cells/axonal projections was evaluated with post hoc histology in all experiments to confirm accurate targeting of BF neurons and a lack of expression in OB neurons as described in^{28,111}. Briefly, mice were deeply anesthetized with an overdose of sodium pentobarbital and perfused with 4% paraformaldehyde in PBS. Tissue sections were evaluated from native fluorescence without immunohistochemical amplification with a Leica TCS SP2 confocal laser scanning microscope at 10x or 20x magnification. The fluorescence intensity of confocal images was analyzed and plotted in ImageJ. Only mice showing a solid OB fiber expression were used for analysis.

For immunohistochemistry animals were perfused as described above. Brains were cryoprotected in 30% sucrose in PBS followed by embedding in optimal cutting temperature compound (Tissue Freezing Medium; Leica). Coronal slices (10–14 μ m) were cut on a cryostat (CM 3050 S, Leica). Slices were first rinsed with PBS and nonspecific binding was blocked with 10% normal goat serum diluted in PBS with 0.2% Triton X-100 for 1 h at room temperature before incubation with primary antibody (rabbit anti-VACHT, 1:300; Synaptic Systems) in PBS with 0.02% Triton-X overnight at 4 °C. As a secondary antibody goat anti-rabbit Alexa Fluor 546 (Invitrogen) was used. The secondary antibody was incubated for 1 h at room temperature before labeling was evaluated as reported above. Colocalization of protein labeling was quantified in ImageJ by manually counting cells from confocal stacks of representative sections at ~Bregma 0.7 in each animal.

Data availability

Data supporting this article have been uploaded as electronic supplementary material.

Received: 15 January 2020; Accepted: 27 May 2020;

Published online: 01 July 2020

References

- Zaborszky, L., Van den Pol, A. N. & Gyengesi, E. In *The Mouse Nervous System* (eds C. Watson, G. Paxinos, & L. Puelles) 684–718 (Elsevier, 2012).
- Sarter, M., Hasselmo, M. E., Bruno, J. P. & Givens, B. Unraveling the attentional functions of cortical cholinergic inputs: interactions between signal-driven and cognitive modulation of signal detection. *Brain Research Reviews* **48**, 98–111 (2005).
- Disney, A. A., Aoki, C. & Hawken, M. J. Gain Modulation by Nicotine in Macaque V1. *Neuron* **56**, 701–713, <https://doi.org/10.1016/j.neuron.2007.09.034> (2007).
- Goard, M. & Dan, Y. Basal forebrain activation enhances cortical coding of natural scenes. *Nat Neurosci* **12**, 1444–1449 (2009).
- Picciotto, M. R., Higley, M. J. & Mineur, Y. S. Acetylcholine as a Neuromodulator: Cholinergic Signaling Shapes Nervous System Function and Behavior. *Neuron* **76**, 116–129, <https://doi.org/10.1016/j.neuron.2012.08.036> (2012).
- Fu, Y. *et al.* A cortical circuit for gain control by behavioral state. *Cell* **156**, 1139–1152, <https://doi.org/10.1016/j.cell.2014.01.050> (2014).
- McGinley, M. J. *et al.* Waking State: Rapid Variations Modulate Neural and Behavioral Responses. *Neuron* **87**, 1143–1161, <https://doi.org/10.1016/j.neuron.2015.09.012> (2015).
- Ogg, M. C., Ross, J. M., Bendahmane, M. & Fletcher, M. L. Olfactory bulb acetylcholine release dishabituates odor responses and reinstates odor investigation. *Nat Commun* **9**, 1868, <https://doi.org/10.1038/s41467-018-04371-w> (2018).
- Thiele, A. & Bellgrove, M. A. Neuromodulation of Attention. *Neuron* **97**, 769–785, <https://doi.org/10.1016/j.neuron.2018.01.008> (2018).
- Zaborszky, L. *et al.* Specific Basal Forebrain-Cortical Cholinergic Circuits Coordinate Cognitive Operations. *J Neurosci* **38**, 9446–9458, <https://doi.org/10.1523/JNEUROSCI.1676-18.2018> (2018).
- Hangya, B., Ranade, S. P., Lorenc, M. & Kepecs, A. Central Cholinergic Neurons Are Rapidly Recruited by Reinforcement Feedback. *Cell* **162**, 1155–1168, <https://doi.org/10.1016/j.cell.2015.07.057> (2015).
- Raver, S. M. & Lin, S. C. Basal forebrain motivational salience signal enhances cortical processing and decision speed. *Front Behav Neurosci* **9**, 277, <https://doi.org/10.3389/fnbeh.2015.00277> (2015).
- Kim, T. *et al.* Cortically projecting basal forebrain parvalbumin neurons regulate cortical gamma band oscillations. *Proc Natl Acad Sci USA* **112**, 3535–3540, <https://doi.org/10.1073/pnas.1413625112> (2015).
- Brown, R. E. & McKenna, J. T. Turning a Negative into a Positive: Ascending GABAergic Control of Cortical Activation and Arousal. *Front Neurol* **6**, 135, <https://doi.org/10.3389/fneur.2015.00135> (2015).

15. Lin, S. C., Brown, R. E., Hussain Shuler, M. G., Petersen, C. C. & Kepecs, A. Optogenetic Dissection of the Basal Forebrain Neuromodulatory Control of Cortical Activation, Plasticity, and Cognition. *J Neurosci* **35**, 13896–13903, <https://doi.org/10.1523/JNEUROSCI.2590-15.2015> (2015).
16. Gritti, I. *et al.* Stereological estimates of the basal forebrain cell population in the rat, including neurons containing choline acetyltransferase, glutamic acid decarboxylase or phosphate-activated glutaminase and colocalizing vesicular glutamate transporters. *Neuroscience* **143**, 1051–1064, <https://doi.org/10.1016/j.neuroscience.2006.09.024> (2006).
17. Henny, P. & Jones, B. E. Projections from basal forebrain to prefrontal cortex comprise cholinergic, GABAergic and glutamatergic inputs to pyramidal cells or interneurons. *Eur J Neurosci* **27**, 654–670, <https://doi.org/10.1111/j.1460-9568.2008.06029.x> (2008).
18. Zaborszky, L. *et al.* Neurons in the basal forebrain project to the cortex in a complex topographic organization that reflects corticocortical connectivity patterns: an experimental study based on retrograde tracing and 3D reconstruction. *Cereb Cortex* **25**, 118–137, <https://doi.org/10.1093/cercor/bht210> (2015).
19. Yang, C., Thankachan, S., McCarley, R. W. & Brown, R. E. The menagerie of the basal forebrain: how many (neural) species are there, what do they look like, how do they behave and who talks to whom? *Curr Opin Neurobiol* **44**, 159–166, <https://doi.org/10.1016/j.conb.2017.05.004> (2017).
20. Busse, L. *et al.* Sensation during Active Behaviors. *J Neurosci* **37**, 10826–10834, <https://doi.org/10.1523/JNEUROSCI.1828-17.2017> (2017).
21. Li, X. *et al.* Generation of a whole-brain atlas for the cholinergic system and mesoscopic projectome analysis of basal forebrain cholinergic neurons. *Proc Natl Acad Sci USA* **115**, 415–420, <https://doi.org/10.1073/pnas.1703601115> (2018).
22. Gielow, M. R. & Zaborszky, L. The Input-Output Relationship of the Cholinergic Basal Forebrain. *Cell Rep* **18**, 1817–1830, <https://doi.org/10.1016/j.celrep.2017.01.060> (2017).
23. Gracia-Llanes, F. J. *et al.* GABAergic basal forebrain afferents innervate selectively GABAergic targets in the main olfactory bulb. *Neuroscience* **170**, 913–922 (2010).
24. Zaborszky, L. *et al.* In *The Rat Nervous System (Fourth Edition)* (ed George Paxinos) 491–507 (Academic Press, 2015).
25. Zaborszky, L., Carlsen, J., Brashear, H. R. & Heimer, L. Cholinergic and GABAergic afferents to the olfactory bulb in the rat with special emphasis on the projection neurons in the nucleus of the horizontal limb of the diagonal band. *J Comp Neurol* **243**, 488–509, <https://doi.org/10.1002/cne.902430405> (1986).
26. Shipley, M. T. & Adamek, G. D. The connections of the mouse olfactory bulb: a study using orthograde and retrograde transport of wheat germ agglutinin conjugated to horseradish peroxidase. *Brain Res Bull* **12**, 669–688 (1984).
27. Ma, M. & Luo, M. Optogenetic Activation of Basal Forebrain Cholinergic Neurons Modulates Neuronal Excitability and Sensory Responses in the Main Olfactory Bulb. *J Neurosci* **32**, 10105–10116, <https://doi.org/10.1523/jneurosci.0058-12.2012> (2012).
28. Rothermel, M., Carey, R. M., Puche, A., Shipley, M. T. & Wachowiak, M. Cholinergic Inputs from Basal Forebrain Add an Excitatory Bias to Odor Coding in the Olfactory Bulb. *The Journal of Neuroscience* **34**, 4654–4664, <https://doi.org/10.1523/jneurosci.5026-13.2014> (2014).
29. Castillo, P. E., Carleton, A., Vincent, J. D. & Lledo, P. M. Multiple and opposing roles of cholinergic transmission in the main olfactory bulb. *J Neurosci* **19**, 9180–9191 (1999).
30. Pignatelli, A. & Belluzzi, O. Cholinergic Modulation of Dopaminergic Neurons in the Mouse Olfactory Bulb. *Chem. Senses* **33**, 331–338, <https://doi.org/10.1093/chemse/bjm091> (2008).
31. Bendahmane, M., Ogg, M. C., Ennis, M. & Fletcher, M. L. Increased olfactory bulb acetylcholine bi-directionally modulates glomerular odor sensitivity. *Sci Rep* **6**, 25808, <https://doi.org/10.1038/srep25808> (2016).
32. Linster, C. & Cleland, T. A. Cholinergic modulation of sensory representations in the olfactory bulb. *Neural Netw* **15**, 709–717 (2002).
33. Chaudhury, D., Escanilla, O. & Linster, C. Bulbar acetylcholine enhances neural and perceptual odor discrimination. *J Neurosci* **29**, 52–60 (2009).
34. de Almeida, L., Idiart, M. & Linster, C. A model of cholinergic modulation in olfactory bulb and piriform cortex. *Journal of Neurophysiology* **109**, 1360–1377, <https://doi.org/10.1152/jn.00577.2012> (2013).
35. Devore, S. & Linster, C. Noradrenergic and cholinergic modulation of olfactory bulb sensory processing. *Front Behav Neurosci* **6**, 52, <https://doi.org/10.3389/fnbeh.2012.00052> (2012).
36. Mandairon, N. *et al.* Cholinergic modulation in the olfactory bulb influences spontaneous olfactory discrimination in adult rats. *European Journal of Neuroscience* **24**, 3234–3244, <https://doi.org/10.1111/j.1460-9568.2006.05212.x> (2006).
37. Fletcher, M. L. & Wilson, D. A. Experience modifies olfactory acuity: acetylcholine-dependent learning decreases behavioral generalization between similar odorants. *J Neurosci* **22**, RC201 (2002).
38. Liu, S. *et al.* Muscarinic receptors modulate dendrodendritic inhibitory synapses to sculpt glomerular output. *J Neurosci* **35**, 5680–5692, <https://doi.org/10.1523/JNEUROSCI.4953-14.2015> (2015).
39. D'Souza, R. D., Parsa, P. V. & Vijayaraghavan, S. Nicotinic receptors modulate olfactory bulb external tufted cells via an excitation-dependent inhibitory mechanism. *Journal of Neurophysiology* **110**, 1544–1553, <https://doi.org/10.1152/jn.00865.2012> (2013).
40. Ghatpande, A. S. & Gelperin, A. Presynaptic Muscarinic Receptors Enhance Glutamate Release at the Mitral/Tufted to Granule Cell Dendrodendritic Synapse in the Rat Main Olfactory Bulb. *J Neurophysiol* **101**, 2052–2061, <https://doi.org/10.1152/jn.90734.2008> (2009).
41. Ravel, N. & Pager, J. Respiratory patterning of the rat olfactory bulb unit activity: nasal versus tracheal breathing. *Neurosci Lett* **115**, 213–218 (1990).
42. D'Souza, R. D. & Vijayaraghavan, S. Nicotinic Receptor-Mediated Filtering of Mitral Cell Responses to Olfactory Nerve Inputs Involves the $\alpha 3\beta 4$ Subtype. *The Journal of Neuroscience* **32**, 3261–3266, <https://doi.org/10.1523/jneurosci.5024-11.2012> (2012).
43. Li, G. & Cleland, T. A. A Two-Layer Biophysical Model of Cholinergic Neuromodulation in Olfactory Bulb. *The Journal of Neuroscience* **33**, 3037–3058, <https://doi.org/10.1523/jneurosci.2831-12.2013> (2013).
44. Ross, J. M., Bendahmane, M. & Fletcher, M. L. Olfactory Bulb Muscarinic Acetylcholine Type 1 Receptors Are Required for Acquisition of Olfactory Fear Learning. *Frontiers in Behavioral Neuroscience* **13**, <https://doi.org/10.3389/fnbeh.2019.00164> (2019).
45. Zheng, Y. *et al.* Different Subgroups of Cholinergic Neurons in the Basal Forebrain Are Distinctly Innervated by the Olfactory Regions and Activated Differentially in Olfactory Memory Retrieval. *Front Neural Circuits* **12**, 99, <https://doi.org/10.3389/fncir.2018.00099> (2018).
46. Soma, S., Shimegi, S., Suematsu, N. & Sato, H. Cholinergic modulation of response gain in the rat primary visual cortex. *Sci Rep* **3**, 1138, <https://doi.org/10.1038/srep01138> (2013).
47. Nunez-Parra, A., Maurer, R. K., Krahe, K., Smith, R. S. & Araneda, R. C. Disruption of centrifugal inhibition to olfactory bulb granule cells impairs olfactory discrimination. *Proc Natl Acad Sci USA* **110**, 14777–14782, <https://doi.org/10.1073/pnas.1310686110> (2013).
48. Sanz Diez, A., Najac, M. & De Saint Jan, D. Basal forebrain GABAergic innervation of olfactory bulb periglomerular interneurons. *J Physiol* **597**, 2547–2563, <https://doi.org/10.1113/JP277811> (2019).
49. Rossi, J. *et al.* Melanocortin-4 receptors expressed by cholinergic neurons regulate energy balance and glucose homeostasis. *Cell Metab* **13**, 195–204, <https://doi.org/10.1016/j.cmet.2011.01.010> (2011).
50. Taniguchi, H. *et al.* A Resource of Cre Driver Lines for Genetic Targeting of GABAergic Neurons in Cerebral Cortex. *Neuron* **71**, 995–1013, <https://doi.org/10.1016/j.neuron.2011.07.026> (2011).

51. Kalmbach, A., Hedrick, T. & Waters, J. Selective optogenetic stimulation of cholinergic axons in neocortex. *Journal of Neurophysiology* **107**, 2008–2019, <https://doi.org/10.1152/jn.00870.2011> (2012).
52. Herman, A. M. *et al.* A cholinergic basal forebrain feeding circuit modulates appetite suppression. *Nature* **538**, 253–256, <https://doi.org/10.1038/nature19789> (2016).
53. Macrides, F., Davis, B. J., Youngs, W. M., Nadi, N. S. & Margolis, F. L. Cholinergic and catecholaminergic afferents to the olfactory bulb in the hamster: a neuroanatomical, biochemical, and histochemical investigation. *J Comp Neurol* **203**, 495–514 (1981).
54. Durand, M., Coronas, V., Jourdan, F. & Quirion, R. Developmental and aging aspects of the cholinergic innervation of the olfactory bulb. *Int J Dev Neurosci* **16**, 777–785, [https://doi.org/10.1016/s0736-5748\(98\)00087-2](https://doi.org/10.1016/s0736-5748(98)00087-2) (1998).
55. Salcedo, E. *et al.* Activity-dependent changes in cholinergic innervation of the mouse olfactory bulb. *PLoS One* **6**, e25441, <https://doi.org/10.1371/journal.pone.0025441> (2011).
56. Gomez, C. *et al.* Heterogeneous targeting of centrifugal inputs to the glomerular layer of the main olfactory bulb. *Journal of Chemical Neuroanatomy* **29**, 238–254 (2005).
57. Carey, R. M. & Wachowiak, M. Effect of sniffing on the temporal structure of mitral/tufted cell output from the olfactory bulb. *J Neurosci* **31**, 10615–10626 (2011).
58. Courtiol, E. *et al.* Reshaping of bulbar odor response by nasal flow rate in the rat. *PLoS One* **6**, e16445, <https://doi.org/10.1371/journal.pone.0016445> (2011).
59. Grosmaître, X., Santarelli, L. C., Tan, J., Luo, M. & Ma, M. Dual functions of mammalian olfactory sensory neurons as odor detectors and mechanical sensors. *Nat Neurosci* **10**, 348–354 (2007).
60. Carey, R. M., Verhagen, J. V., Wesson, D. W., Pirez, N. & Wachowiak, M. Temporal Structure of Receptor Neuron Input to the Olfactory Bulb Imaged in Behaving Rats. *J Neurophysiol* **101**, 1073–1088, <https://doi.org/10.1152/jn.90902.2008> (2009).
61. Linster, C. & Hasselmo, M. E. Neural activity in the horizontal limb of the diagonal band of Broca can be modulated by electrical stimulation of the olfactory bulb and cortex in rats. *Neurosci Lett* **282**, 157–160 (2000).
62. Detari, L. & Vanderwolf, C. H. Activity of identified cortically projecting and other basal forebrain neurones during large slow waves and cortical activation in anaesthetized rats. *Brain Res* **437**, 1–8 (1987).
63. Manns, I. D., Alonso, A. & Jones, B. E. Rhythmically discharging basal forebrain units comprise cholinergic, GABAergic, and putative glutamatergic cells. *J Neurophysiol* **89**, 1057–1066, <https://doi.org/10.1152/jn.00938.2002> (2003).
64. Hassani, O. K., Lee, M. G., Henny, P. & Jones, B. E. Discharge Profiles of Identified GABAergic in Comparison to Cholinergic and Putative Glutamatergic Basal Forebrain Neurons across the Sleep-Wake Cycle. *Journal of Neuroscience* **29**, 11828–11840, <https://doi.org/10.1523/JNEUROSCI.1259-09.2009> (2009).
65. Voytko, M. L. *et al.* Basal forebrain lesions in monkeys disrupt attention but not learning and memory. *J Neurosci* **14**, 167–186 (1994).
66. Martinez, V., Parikh, V. & Sarter, M. Sensitized attentional performance and Fos-immunoreactive cholinergic neurons in the basal forebrain of amphetamine-pretreated rats. *Biol Psychiatry* **57**, 1138–1146, <https://doi.org/10.1016/j.biopsych.2005.02.005> (2005).
67. Fuller, P. M., Sherman, D., Pedersen, N. P., Saper, C. B. & Lu, J. Reassessment of the structural basis of the ascending arousal system. *J Comp Neurol* **519**, 933–956, <https://doi.org/10.1002/cne.22559> (2011).
68. Brown, R. E., Basheer, R., McKenna, J. T., Strecker, R. E. & McCarley, R. W. Control of sleep and wakefulness. *Physiol Rev* **92**, 1087–1187, <https://doi.org/10.1152/physrev.00032.2011> (2012).
69. Anaclet, C. *et al.* Basal forebrain control of wakefulness and cortical rhythms. *Nat Commun* **6**, 8744, <https://doi.org/10.1038/ncomms9744> (2015).
70. Cohen, M. R. & Maunsell, J. H. Attention improves performance primarily by reducing interneuronal correlations. *Nat Neurosci* **12**, 1594–1600, <https://doi.org/10.1038/nn.2439> (2009).
71. Pinto, L. *et al.* Fast modulation of visual perception by basal forebrain cholinergic neurons. *Nat Neurosci* **16**, 1857–1863, <https://doi.org/10.1038/nn.3552> (2013).
72. Chen, N., Sugihara, H. & Sur, M. An acetylcholine-activated microcircuit drives temporal dynamics of cortical activity. *Nat Neurosci* **18**, 892–902, <https://doi.org/10.1038/nn.4002> (2015).
73. Runfeldt, M. J., Sadovsky, A. J. & MacLean, J. N. Acetylcholine functionally reorganizes neocortical microcircuits. *J Neurophysiol* **112**, 1205–1216, <https://doi.org/10.1152/jn.00071.2014> (2014).
74. Thiele, A., Herrero, J. L., Distler, C. & Hoffmann, K. P. Contribution of cholinergic and GABAergic mechanisms to direction tuning, discriminability, response reliability, and neuronal rate correlations in macaque middle temporal area. *J Neurosci* **32**, 16602–16615, <https://doi.org/10.1523/JNEUROSCI.0554-12.2012> (2012).
75. Nelson, A. & Mooney, R. The Basal Forebrain and Motor Cortex Provide Convergent yet Distinct Movement-Related Inputs to the Auditory Cortex. *Neuron* **90**, 635–648, <https://doi.org/10.1016/j.neuron.2016.03.031> (2016).
76. Do, J. P. *et al.* Cell type-specific long-range connections of basal forebrain circuit. *Elife* **5**, <https://doi.org/10.7554/eLife.13214> (2016).
77. Agostinelli, L. J., Geerling, J. C. & Scammell, T. E. Basal forebrain subcortical projections. *Brain Struct Funct* **224**, 1097–1117, <https://doi.org/10.1007/s00429-018-01820-6> (2019).
78. Hasselmo, M. E. & Schnell, E. Laminar selectivity of the cholinergic suppression of synaptic transmission in rat hippocampal region CA1: computational modeling and brain slice physiology. *J Neurosci* **14**, 3898–3914 (1994).
79. Tian, M. K., Bailey, C. D. & Lambe, E. K. Cholinergic excitation in mouse primary vs. associative cortex: region-specific magnitude and receptor balance. *Eur J Neurosci* **40**, 2608–2618, <https://doi.org/10.1111/ejn.12622> (2014).
80. Chaves-Coira, I., Barros-Zulaica, N., Rodrigo-Angulo, M. & Nunez, A. Modulation of Specific Sensory Cortical Areas by Segregated Basal Forebrain Cholinergic Neurons Demonstrated by Neuronal Tracing and Optogenetic Stimulation in Mice. *Front Neural Circuits* **10**, 28, <https://doi.org/10.3389/fncir.2016.00028> (2016).
81. Chaves-Coira, I., Martin-Cortecero, J., Nunez, A. & Rodrigo-Angulo, M. L. Basal Forebrain Nuclei Display Distinct Projecting Pathways and Functional Circuits to Sensory Primary and Prefrontal Cortices in the Rat. *Front Neuroanat* **12**, 69, <https://doi.org/10.3389/fnana.2018.00069> (2018).
82. Chaves-Coira, I., Rodrigo-Angulo, M. L. & Nunez, A. Bilateral Pathways from the Basal Forebrain to Sensory Cortices May Contribute to Synchronous Sensory Processing. *Front Neuroanat* **12**, 5, <https://doi.org/10.3389/fnana.2018.00005> (2018).
83. Case, D. T. *et al.* Layer- and cell type-selective co-transmission by a basal forebrain cholinergic projection to the olfactory bulb. *Nat Commun* **8**, 652, <https://doi.org/10.1038/s41467-017-00765-4> (2017).
84. Foutz, T. J., Arlow, R. L. & McIntyre, C. C. Theoretical principles underlying optical stimulation of a channelrhodopsin-2 positive pyramidal neuron. *J Neurophysiol* **107**, 3235–3245, <https://doi.org/10.1152/jn.00501.2011> (2012).
85. Woolf, N. J., Eckenstein, F. & Butcher, L. L. Cholinergic systems in the rat brain: I. projections to the limbic telencephalon. *Brain Res Bull* **13**, 751–784 (1984).
86. Carlsen, J., Zaborszky, L. & Heimer, L. Cholinergic projections from the basal forebrain to the basolateral amygdaloid complex: a combined retrograde fluorescent and immunohistochemical study. *J Comp Neurol* **234**, 155–167, <https://doi.org/10.1002/cne.902340203> (1985).
87. Linster, C., Wyble, B. P. & Hasselmo, M. E. Electrical stimulation of the horizontal limb of the diagonal band of Broca modulates population EPSPs in piriform cortex. *J Neurophysiol* **81**, 2737–2742 (1999).
88. Zimmer, L. A., Ennis, M. & Shipley, M. T. Diagonal band stimulation increases piriform cortex neuronal excitability *in vivo*. *Neuroreport* **10**, 2101–2105 (1999).

89. Boyd, A. M., Sturgill, J. F., Poo, C. & Isaacson, J. S. Cortical feedback control of olfactory bulb circuits. *Neuron* **76**, 1161–1174, <https://doi.org/10.1016/j.neuron.2012.10.020> (2012).
90. Markopoulos, F., Rokni, D., Gire, D. H. & Murthy, V. N. Functional properties of cortical feedback projections to the olfactory bulb. *Neuron* **76**, 1175–1188, <https://doi.org/10.1016/j.neuron.2012.10.028> (2012).
91. Otazu, G. H., Chae, H., Davis, M. B. & Albeanu, D. F. Cortical Feedback Decorrelates Olfactory Bulb Output in Awake Mice. *Neuron* **86**, 1461–1477, <https://doi.org/10.1016/j.neuron.2015.05.023> (2015).
92. Gritti, I., Manns, I. D., Mainville, L. & Jones, B. E. Parvalbumin, calbindin, or calretinin in cortically projecting and GABAergic, cholinergic, or glutamatergic basal forebrain neurons of the rat. *J Comp Neurol* **458**, 11–31, <https://doi.org/10.1002/cne.10505> (2003).
93. McKenna, J. T. *et al.* Distribution and intrinsic membrane properties of basal forebrain GABAergic and parvalbumin neurons in the mouse. *J Comp Neurol* **521**, 1225–1250, <https://doi.org/10.1002/cne.23290> (2013).
94. Zaborszky, L. & Duque, A. Local synaptic connections of basal forebrain neurons. *Behavioural Brain Research* **115**, 143–158, [https://doi.org/10.1016/S0166-4328\(00\)00255-2](https://doi.org/10.1016/S0166-4328(00)00255-2) (2000).
95. Yang, C. *et al.* Cholinergic Neurons Excite Cortically Projecting Basal Forebrain GABAergic Neurons. *The Journal of Neuroscience* **34**, 2832–2844, <https://doi.org/10.1523/jneurosci.3235-13.2014> (2014).
96. Dannenberg, H. *et al.* Synergy of direct and indirect cholinergic septo-hippocampal pathways coordinates firing in hippocampal networks. *J Neurosci* **35**, 8394–8410, <https://doi.org/10.1523/JNEUROSCI.4460-14.2015> (2015).
97. Ren, J. *et al.* Habenula Cholinergic Neurons Corelease Glutamate and Acetylcholine and Activate Postsynaptic Neurons via Distinct Transmission Modes. *Neuron* **69**, 445–452 (2011).
98. D'Souza, R. D. & Vijayaraghavan, S. Paying attention to smell: cholinergic signaling in the olfactory bulb. *Front Synaptic Neurosci* **6**, 21, <https://doi.org/10.3389/fnsyn.2014.00021> (2014).
99. Lendvai, B. & Vizi, E. S. Nonsynaptic chemical transmission through nicotinic acetylcholine receptors. *Physiol Rev* **88**, 333–349, <https://doi.org/10.1152/physrev.00040.2006> (2008).
100. Le Jeune, H., Aubert, I., Jourdan, F. & Quirion, R. Comparative laminar distribution of various autoradiographic cholinergic markers in adult rat main olfactory bulb. *Journal of Chemical Neuroanatomy* **9**, 99–112 (1995).
101. Keiger, C. J. & Walker, J. C. Individual variation in the expression profiles of nicotinic receptors in the olfactory bulb and trigeminal ganglion and identification of alpha2, alpha6, alpha9, and beta3 transcripts. *Biochem Pharmacol* **59**, 233–240, [https://doi.org/10.1016/S0006-2952\(99\)00326-3](https://doi.org/10.1016/S0006-2952(99)00326-3) (2000).
102. Pressler, R. T., Inoue, T. & Strowbridge, B. W. Muscarinic receptor activation modulates granule cell excitability and potentiates inhibition onto mitral cells in the rat olfactory bulb. *J Neurosci* **27**, 10969–10981 (2007).
103. De Saint Jan, D., Hirnet, D., Westbrook, G. L. & Charpak, S. External Tufted Cells Drive the Output of Olfactory Bulb Glomeruli. *J. Neurosci.* **29**, 2043–2052, <https://doi.org/10.1523/jneurosci.5317-08.2009> (2009).
104. Najac, M., De Saint Jan, D., Reguero, L., Grandes, P. & Charpak, S. Monosynaptic and Polysynaptic Feed-Forward Inputs to Mitral Cells from Olfactory Sensory Neurons. *The Journal of Neuroscience* **31**, 8722–8729, <https://doi.org/10.1523/jneurosci.0527-11.2011> (2011).
105. Gire, D. H. *et al.* Mitral Cells in the Olfactory Bulb Are Mainly Excited through a Multistep Signaling Path. *The Journal of Neuroscience* **32**, 2964–2975, <https://doi.org/10.1523/jneurosci.5580-11.2012> (2012).
106. Caputi, A., Melzer, S., Michael, M. & Monyer, H. The long and short of GABAergic neurons. *Curr Opin Neurobiol* **23**, 179–186, <https://doi.org/10.1016/j.conb.2013.01.021> (2013).
107. Short, S. M. & Wachowiak, M. Temporal dynamics of inhalation-linked activity across defined subpopulations of mouse olfactory bulb neurons imaged *in vivo*. *bioRxiv*, 558999, <https://doi.org/10.1101/558999> (2019).
108. Nagayama, S., Homma, R. & Imamura, F. Neuronal organization of olfactory bulb circuits. *Front Neural Circuits* **8**, 98, <https://doi.org/10.3389/fncir.2014.00098> (2014).
109. McDonald, A. J., Muller, J. F. & Mascagni, F. Postsynaptic targets of GABAergic basal forebrain projections to the basolateral amygdala. *Neuroscience* **183**, 144–159, <https://doi.org/10.1016/j.neuroscience.2011.03.027> (2011).
110. Kato, H. K., Chu, M. W., Isaacson, J. S. & Komiyama, T. Dynamic sensory representations in the olfactory bulb: modulation by wakefulness and experience. *Neuron* **76**, 962–975, <https://doi.org/10.1016/j.neuron.2012.09.037> (2012).
111. Wachowiak, M. *et al.* Optical Dissection of Odor Information Processing *In Vivo* Using GCaMPs Expressed in Specified Cell Types of the Olfactory Bulb. *J Neurosci* **33**, 5285–5300, <https://doi.org/10.1523/jneurosci.4824-12.2013> (2013).
112. Youngstrom, I. A. & Strowbridge, B. W. Respiratory modulation of spontaneous subthreshold synaptic activity in olfactory bulb granule cells recorded in awake, head-fixed mice. *J Neurosci* **35**, 8758–8767, <https://doi.org/10.1523/JNEUROSCI.0311-15.2015> (2015).
113. Xu, M. *et al.* Basal forebrain circuit for sleep-wake control. *Nat Neurosci* **18**, 1641–1647, <https://doi.org/10.1038/nn.4143> (2015).
114. Harrison, T. C., Pinto, L., Brock, J. R. & Dan, Y. Calcium Imaging of Basal Forebrain Activity during Innate and Learned Behaviors. *Front Neural Circuits* **10**, 36, <https://doi.org/10.3389/fncir.2016.00036> (2016).
115. Paolini, A. G. & McKenzie, J. S. Intracellular recording of magnocellular preoptic neuron responses to olfactory brain. *Neuroscience* **78**, 229–242, [https://doi.org/10.1016/S0306-4522\(96\)00566-0](https://doi.org/10.1016/S0306-4522(96)00566-0) (1997).
116. Rothermel, M. & Wachowiak, M. Functional imaging of cortical feedback projections to the olfactory bulb. *Front Neural Circuits* **8**, 73, <https://doi.org/10.3389/fncir.2014.00073> (2014).
117. Bozza, T., McGann, J. P., Mombaerts, P. & Wachowiak, M. *In vivo* imaging of neuronal activity by targeted expression of a genetically encoded probe in the mouse. *Neuron* **42**, 9–21 (2004).
118. Verhagen, J. V., Wesson, D. W., Netoff, T. L., White, J. A. & Wachowiak, M. Sniffing controls an adaptive filter of sensory input to the olfactory bulb. *Nat Neurosci* **10**, 631–639 (2007).
119. Wachowiak, M. & Cohen, L. B. Representation of odorants by receptor neuron input to the mouse olfactory bulb. *Neuron* **32**, 723–735 (2001).
120. Spors, H., Wachowiak, M., Cohen, L. B. & Friedrich, R. W. Temporal dynamics and latency patterns of receptor neuron input to the olfactory bulb. *J Neurosci* **26**, 1247–1259 (2006).
121. Eiting, T. P. & Wachowiak, M. Artificial Inhalation Protocol in Adult Mice. *Bio Protoc* **8**, <https://doi.org/10.21769/BioProtoc.3024> (2018).
122. Lewicki, M. S. A review of methods for spike sorting: the detection and classification of neural action potentials. *Network* **9**, R53–78 (1998).

Acknowledgements

The authors thank the technical workshop at the institute for biology II, RWTH Aachen for excellent technical support. We thank all lab members for helpful discussions and comments on the manuscript. We thank R. Medinaceli Quintela, L. Wallhorn, V. Schweda, J. Koesling, and N. Rose for assistance with optogenetics experiments, especially in the early project phase. Initial data were acquired in Utah. We thank Drs. Looger, Akerboom, and Kim and the Genetically Encoded Calcium Indicator (GECI) Project at Janelia Farm Research Campus in collaboration with Penn Vector Core for providing opsin-expressing viruses. This work was funded

by the Deutsche Forschungsgemeinschaft (DFG, German Research Foundation) - (RO 4046/2-1 and /2-2, Emmy Noether Program [to MR] and the Research Training Group 2416 “MultiSenses – MultiScales: Novel approaches to decipher neural processing in multisensory integration” 368482240/GRK2416) and by a grant from the Interdisciplinary Centre for Clinical Research within the faculty of Medicine at the RWTH Aachen University (IZKF TN1-7 532007).

Author contributions

E.B. performed experiments and analyzed data; D.B. and M.R. designed experiments, analyzed data and wrote the manuscript

Competing interests

The authors declare no competing interests.

Additional information

Supplementary information is available for this paper at <https://doi.org/10.1038/s41598-020-67276-z>.

Correspondence and requests for materials should be addressed to M.R.

Reprints and permissions information is available at www.nature.com/reprints.

Publisher’s note Springer Nature remains neutral with regard to jurisdictional claims in published maps and institutional affiliations.



Open Access This article is licensed under a Creative Commons Attribution 4.0 International License, which permits use, sharing, adaptation, distribution and reproduction in any medium or format, as long as you give appropriate credit to the original author(s) and the source, provide a link to the Creative Commons license, and indicate if changes were made. The images or other third party material in this article are included in the article’s Creative Commons license, unless indicated otherwise in a credit line to the material. If material is not included in the article’s Creative Commons license and your intended use is not permitted by statutory regulation or exceeds the permitted use, you will need to obtain permission directly from the copyright holder. To view a copy of this license, visit <http://creativecommons.org/licenses/by/4.0/>.

© The Author(s) 2020